Towards the theory of ferrimagnetism: II

2009 J. Phys.: Condens. Matter 21 216003

(http://iopscience.iop.org/0953-8984/21/21/216003)

J. Phys.: Condens. Matter **21** (2009) 216003 (9pp) doi:10.1088/0953-8984/21/21/216003

Towards the theory of ferrimagnetism: II

Naoum Karchev

Department of Physics, University of Sofia, 1126 Sofia, Bulgaria

Received 13 January 2009, in final form 20 March 2009
Published 29 April 2009
Online at stacks.iop.org/JPhysCM/21/216003

Abstract

The present paper is a sequel to the paper by Karchev (2008 *J. Phys.: Condens. Matter* **20** 325219). A two-sublattice ferrimagnet, with spin-s_1 operators $\mathbf{S}_{1i}$ at the sublattice A site and spin-s_2 operators $\mathbf{S}_{2i}$ at the sublattice B site, is considered. Renormalized spin-wave theory, which accounts for the magnon–magnon interaction, and its extension are developed to describe the two ferrimagnetic phases $(0, T^*)$ and (T^*, T_N) in the system, and to calculate the magnetization as a function of temperature.

The influence of the parameters in the theory on the characteristic temperatures T_N and T^* is studied. It is shown that, increasing the inter-sublattice exchange interaction, the ratio $T_N/T^* > 1$ decreases approaching one, and above some critical value of the exchange constant there is only one phase $T_N = T^*$, and the magnetization–temperature curve has the typical Curie–Weiss profile. When the intra-exchange constant of the sublattice with stronger intra-exchange interaction increases the Néel temperature increases while T^* remains unchanged. Finally, when the magnetic order of the sublattice with smaller magnetic order decreases, T^* decreases. The theoretical predictions are utilized to interpret the experimentally measured magnetization–temperature curves.

(Some figures in this article are in colour only in the electronic version)

1. Introduction

The present paper is a sequel to the paper [1]. A two-sublattice ferrimagnet, with spin-s_1 operators $\mathbf{S}_{1i}$ at the sublattice A site and spin-s_2 operators $\mathbf{S}_{2i}$ at the sublattice B site. The true magnons of a two-spin system are transversal fluctuations of the total magnetization which includes both the magnetization of the sublattice A and B spins. The magnon excitation is a complicated mixture of the transversal fluctuations of the sublattice A and B spins. As a result the magnons' fluctuations suppress, in different ways, the magnetic orders on the different sublattices and one obtains two phases. At low temperature $(0, T^*)$ the magnetic orders of the A and B spins contribute to the magnetization of the system, while at high temperature (T^*, T_N) the magnetization of the spins with a weaker intra-sublattice exchange is suppressed by magnon fluctuations, and only the spins with the stronger intra-sublattice exchange have non-zero spontaneous magnetization.

Renormalized spin-wave theory, which accounts for the magnon–magnon interaction, and its extension are developed to describe the two ferrimagnetic phases in the system and to calculate the magnetization as a function of temperature. It is impossible to require the theoretically calculated Néel temperature and magnetization–temperature curves to be in exact accordance with experimental results. The models are idealized, and they do not consider many important effects: phonon modes, several types of disorder, Coulomb interaction, etc. Because of this it is important to formulate theoretical criteria for the adequacy of the method of calculation. In my opinion the calculations should be in accordance with the Mermin–Wagner theorem [2]. It claims that in two dimensions there is no spontaneous magnetization at non-zero temperature. Hence, the critical temperature should be equal to zero. It is well known that the Monte Carlo method of calculation does not satisfy this criteria, and a 'weak z coupling' 3D system is used to mimic a 2D layer. It is difficult within dynamical mean-field theory (DMFT) to make a difference between two-dimensional and three-dimensional systems. DMFT is a good approximation when the dimensionality goes to infinity. The present methods of calculation, being approximate, capture the basic physical features and satisfy the Mermin–Wagner theorem.

There is an important difference between Néel theory [3] and the results in the present paper. Néel's calculations predict a temperature T_N at which both the sublattice A and B magnetizations become equal to zero and T^* is a temperature at which the magnetic moment has a maximum.

The influence of the parameters in the theory on the characteristic temperatures T_N and T^* is studied. It is shown that, increasing the inter-sublattice exchange interaction, the

ratio $T_N/T^* > 1$ decreases approaching one, and above some critical value of the exchange constant there is only one phase $T_N = T^*$, and the magnetization–temperature curve has the typical Curie–Weiss profile. When the intra-exchange constant of the sublattice with stronger intra-exchange interaction increases the Néel temperature increases while T^* remains unchanged. Finally, when the magnetic order of the sublattice with smaller magnetic order decreases, T^* decreases.

To compare the theoretical results and the experimental magnetization–temperature curves one has, first of all, to interpret adequately the measurements. The magnetic moments in some materials are close to the 'spin-only' value $2\mu_B S$ and the sublattice spins s_1 and s_2 can be obtained from the experimental curves. As an example I consider the sulfo-spinel $MnCr_2S_{4-x}Se_x$ [4]. On the other hand there are ferrimagnets with strong spin–orbital interaction. It is convenient, in that case, to consider jj coupling with $\mathbf{J}^A = \mathbf{L}^A + \mathbf{S}^A$ and $\mathbf{J}^B = \mathbf{L}^B + \mathbf{S}^B$. As an example I consider the vanadium spinel MnV_2O_4 [5–8].

This paper is organized as follows. In section 2 the model is presented and a renormalized spin-wave theory is worked out to calculate the magnetization–temperature curves for different parameters of the model. The influence of the theoretical parameters on the Néel and T^* temperatures is studied in section 3. I consider three cases: (i) when the inter-sublattice exchange constant increases and all the other parameters are fixed, (ii) one of the intra-sublattice parameters is changed and (iii) when one of the spins decreases. Applications and analyses of the experimental magnetization–temperature curves are given in section 4. A summary in section 5 concludes the paper.

2. Spin-wave theory

2.1. Renormalized spin-wave (RSW) theory

The Hamiltonian of the system is

$$H = -J_1 \sum_{\langle\langle ij\rangle\rangle_A} \mathbf{S}_{1i}\cdot\mathbf{S}_{1j} - J_2 \sum_{\langle\langle ij\rangle\rangle_B} \mathbf{S}_{2i}\cdot\mathbf{S}_{2j} + J\sum_{\langle ij\rangle}\mathbf{S}_{1i}\cdot\mathbf{S}_{2j} \tag{1}$$

where the sums are over all sites of a three-dimensional cubic lattice: $\langle i, j\rangle$ denotes the sum over the nearest neighbors, $\langle\langle i, j\rangle\rangle_A$ denotes the sum over the sites of the A sublattice and $\langle\langle i, j\rangle\rangle_B$ denotes the sum over the sites of the B sublattice. The first two terms describe the ferromagnetic Heisenberg intra-sublattice exchange $J_1 > 0, J_2 > 0$, while the third term describes the inter-sublattice exchange which is antiferromagnetic $J > 0$. To study a theory with the Hamiltonian equation (1) it is convenient to introduce the Holstein–Primakoff representation for the spin operators:

$$\begin{aligned} S^+_{1j} &= S^1_{1j} + iS^2_{1j} = \sqrt{2s_1 - a^+_j a_j}\,a_j \\ S^-_{1j} &= S^1_{1j} - iS^2_{1j} = a^+_j\sqrt{2s_1 - a^+_j a_j} \\ S^3_{1j} &= s_1 - a^+_j a_j \end{aligned} \tag{2}$$

when the sites j are from sublattice A and

$$\begin{aligned} S^+_{2j} &= S^1_{2j} + iS^2_{2j} = -b^+_j\sqrt{2s_2 - b^+_j b_j} \\ S^-_{2j} &= S^1_{2j} - iS^2_{2j} = -\sqrt{2s_2 - b^+_j b_j}\,b_j \\ S^3_{2j} &= -s_2 + b^+_j b_j \end{aligned} \tag{3}$$

when the sites j are from sublattice B. The operators a^+_j, a_j and b^+_j, b_j satisfy the Bose commutation relations. In terms of the Bose operators and keeping only the quadratic and quartic terms, the effective Hamiltonian equation (1) adopts the form

$$H = H_2 + H_4 \tag{4}$$

where

$$\begin{aligned} H_2 = {} & s_1 J_1 \sum_{\langle\langle ij\rangle\rangle_A} (a^+_i a_i + a^+_j a_j - a^+_j a_i - a^+_i a_j) \\ & + s_2 J_2 \sum_{\langle\langle ij\rangle\rangle_B} (b^+_i b_i + b^+_j b_j - b^+_j b_i - b^+_i b_j) \\ & + J\sum_{\langle ij\rangle}[s_1 b^+_j b_j + s_2 a^+_i a_i - \sqrt{s_1 s_2}(a^+_i b^+_j + a_i b_j)] \end{aligned} \tag{5}$$

$$\begin{aligned} H_4 = {} & \tfrac{1}{4} J_1 \sum_{\langle\langle ij\rangle\rangle_A} [a^+_i a^+_j (a_i - a_j)^2 + (a^+_i - a^+_j)^2 a_i a_j] \\ & + \tfrac{1}{4} J_2 \sum_{\langle\langle ij\rangle\rangle_B} [b^+_i b^+_j (b_i - b_j)^2 + (b^+_i - b^+_j)^2 b_i b_j] \\ & + \frac{1}{4} J \sum_{\langle ij\rangle}\Bigg[\sqrt{\frac{s_1}{s_2}}(a_i b^+_j b_j b_j + a^+_i b^+_j b^+_j b_j) \\ & + \sqrt{\frac{s_2}{s_1}}(a^+_i a_i a_i b_j + a^+_i a^+_i a_i b^+_j) - 4a^+_i a_i b^+_j b_j\Bigg] \end{aligned} \tag{6}$$

and the terms without operators are dropped.

The next step is to represent the Hamiltonian in the Hartree–Fock approximation:

$$H \approx H_{HF} = H_{cl} + H_q \tag{7}$$

where

$$\begin{aligned} H_{cl} = {} & 12NJ_1 s_1^2 (u_1 - 1)^2 + 12NJ_2 s_2^2 (u_2 - 1)^2 \\ & + 6NJ s_1 s_2 (u - 1)^2, \end{aligned} \tag{8}$$

$$\begin{aligned} H_2 = {} & s_1 J_1 u_1 \sum_{\langle\langle ij\rangle\rangle_A} (a^+_i a_i + a^+_j a_j - a^+_j a_i - a^+_i a_j) \\ & + s_2 J_2 u_2 \sum_{\langle\langle ij\rangle\rangle_B} (b^+_i b_i + b^+_j b_j - b^+_j b_i - b^+_i b_j) \\ & + Ju\sum_{\langle ij\rangle}[s_1 b^+_j b_j + s_2 a^+_i a_i - \sqrt{s_1 s_2}(a^+_i b^+_j + a_i b_j)] \end{aligned} \tag{9}$$

and $N = N_A = N_B$ is the number of sites on a sublattice. Equation (9) shows that the Hartree–Fock parameters u_1, u_2 and u renormalize the intra-exchange constants J_1, J_2 and the inter-exchange constant J, respectively.

It is convenient to rewrite the Hamiltonian in the momentum space representation:

$$H_q = \sum_{k\in B_r}[\varepsilon^a_k a^+_k a_k + \varepsilon^b_k b^+_k b_k - \gamma_k(a^+_k b^+_k + b_k a_k)], \tag{10}$$

where the wavevector k runs over the reduced first Brillouin zone B_r of a cubic lattice. The dispersions are given by the equalities

$$\begin{aligned}\varepsilon_k^a &= 4s_1J_1u_1\varepsilon_k + 6s_2Ju\\ \varepsilon_k^b &= 4s_2J_2u_2\varepsilon_k + 6s_1Ju\\ \gamma_k &= 2Ju\sqrt{s_1s_2}(\cos k_x + \cos k_y + \cos k_z)\end{aligned} \tag{11}$$

with

$$\begin{aligned}\varepsilon_k = 6 &- \cos(k_x + k_y) - \cos(k_x - k_y) - \cos(k_x + k_z)\\ &- \cos(k_x - k_z) - \cos(k_y + k_z) - \cos(k_y - k_z).\end{aligned} \tag{12}$$

To diagonalize the Hamiltonian one introduces new Bose fields $\alpha_k, \alpha_k^+, \beta_k, \beta_k^+$ by means of the transformation

$$\begin{aligned}a_k &= u_k\alpha_k + v_k\beta_k^+ \qquad a_k^+ = u_k\alpha_k^+ + v_k\beta_k\\ b_k &= u_k\beta_k + v_k\alpha_k^+ \qquad b_k^+ = u_k\beta_k^+ + v_k\alpha_k\end{aligned} \tag{13}$$

where the coefficients of the transformation u_k and v_k are real functions of the wavevector k:

$$\begin{aligned}u_k &= \sqrt{\frac{1}{2}\left(\frac{\varepsilon_k^a + \varepsilon_k^b}{\sqrt{(\varepsilon_k^a + \varepsilon_k^b)^2 - 4\gamma_k^2}} + 1\right)}\\ v_k &= \mathrm{sgn}(\gamma_k)\sqrt{\frac{1}{2}\left(\frac{\varepsilon_k^a + \varepsilon_k^b}{\sqrt{(\varepsilon_k^a + \varepsilon_k^b)^2 - 4\gamma_k^2}} - 1\right)}.\end{aligned} \tag{14}$$

The transformed Hamiltonian adopts the form

$$H_q = \sum_{k\in B_r}(E_k^\alpha\alpha_k^+\alpha_k + E_k^\beta\beta_k^+\beta_k + E_k^0), \tag{15}$$

with new dispersions

$$\begin{aligned}E_k^\alpha &= \tfrac{1}{2}\left[\sqrt{(\varepsilon_k^a + \varepsilon_k^b)^2 - 4\gamma_k^2} - \varepsilon_k^b + \varepsilon_k^a\right]\\ E_k^\beta &= \tfrac{1}{2}\left[\sqrt{(\varepsilon_k^a + \varepsilon_k^b)^2 - 4\gamma_k^2} + \varepsilon_k^b - \varepsilon_k^a\right]\end{aligned} \tag{16}$$

and vacuum energy

$$E_k^0 = \tfrac{1}{2}\left[\sqrt{(\varepsilon_k^a + \varepsilon_k^b)^2 - 4\gamma_k^2} - \varepsilon_k^b - \varepsilon_k^a\right]. \tag{17}$$

For positive values of the Hartree–Fock parameters and all values of $k \in B_r$, the dispersions are nonnegative $E_k^\alpha \geqslant 0, E_k^\beta \geqslant 0$. For definiteness I choose $s_1 > s_2$. With these parameters, the α_k boson is the long-range *(magnon)* excitation in the two-spin system with $E_k^\alpha \propto \rho k^2$, near the zero wavevector, while the β_k boson is a gapped excitation.

To obtain the system of equations for the Hartree–Fock parameters we consider the free energy of a system with Hamiltonian H_{HF} equations (8) and (15):

$$\begin{aligned}\mathcal{F} = &12J_1s_1^2(u_1 - 1)^2 + 12J_2s_2^2(u_2 - 1)^2\\ &+ 6Js_1s_2(u - 1)^2 + \frac{1}{N}\sum_{k\in B_r}E_k^0 + \frac{1}{\beta N}\\ &\times\sum_{k\in B_r}[\ln(1 - \mathrm{e}^{-\beta E_k^\alpha}) + \ln(1 - \mathrm{e}^{-\beta E_k^\beta})]\end{aligned} \tag{18}$$

where $\beta = 1/T$ is the inverse temperature. Then the three equations

$$\partial\mathcal{F}/\partial u_1 = 0, \qquad \partial\mathcal{F}/\partial u_2 = 0, \qquad \partial\mathcal{F}/\partial u = 0 \tag{19}$$

adopt the form (see the appendix)

$$\begin{aligned}u_1 &= 1 - \frac{1}{6s_1}\frac{1}{N}\sum_{k\in B_r}\varepsilon_k[u_k^2n_k^\alpha + v_k^2n_k^\beta + v_k^2]\\ u_2 &= 1 - \frac{1}{6s_2}\frac{1}{N}\sum_{k\in B_r}\varepsilon_k[v_k^2n_k^\alpha + u_k^2n_k^\beta + v_k^2]\\ u &= 1 - \frac{1}{N}\sum_{k\in B_r}\left[\frac{1}{2s_1}(u_k^2n_k^\alpha + v_k^2n_k^\beta + v_k^2)\right.\\ &\quad + \frac{1}{2s_2}(v_k^2n_k^\alpha + u_k^2n_k^\beta + v_k^2)\\ &\quad \left. - \frac{2}{3}Ju(1 + n_k^\alpha + n_k^\beta)\frac{(\cos k_x + \cos k_y + \cos k_z)^2}{\sqrt{(\varepsilon_k^a + \varepsilon_k^b)^2 - 4\gamma_k^2}}\right]\end{aligned} \tag{20}$$

where n_k^α and n_k^β are the Bose functions of α and β excitations. The Hartree–Fock parameters, the solution of the system of equations (20), are positive functions of T/J, $u_1(T/J) > 0, u_2(T/J) > 0$ and $u(T/J) > 0$. Utilizing these functions, one can calculate the spontaneous magnetization of the system, which is a sum of the spontaneous magnetization on the two sublattices $M = M^A + M^B$, where

$$\begin{aligned}M^A &= \langle S_{1j}^3\rangle \qquad j \text{ is from sublattice A}\\ M^B &= \langle S_{2j}^3\rangle \qquad j \text{ is from sublattice B.}\end{aligned} \tag{21}$$

In terms of the Bose functions of the α and β excitations they adopt the form

$$\begin{aligned}M^A &= s_1 - \frac{1}{N}\sum_{k\in B_r}[u_k^2n_k^\alpha + v_k^2n_k^\beta + v_k^2]\\ M^B &= -s_2 + \frac{1}{N}\sum_{k\in B_r}[v_k^2n_k^\alpha + u_k^2n_k^\beta + v_k^2].\end{aligned} \tag{22}$$

The magnon excitation—α_k in the effective theory equation (15)—is a complicated mixture of the transversal fluctuations of the A and B spins. As a result the magnons' fluctuations suppress in a different way the magnetization on sublattices A and B. Quantitatively this depends on the coefficients u_k and v_k in equations (22). At characteristic temperature T^* spontaneous magnetization on sublattice B becomes equal to zero, while spontaneous magnetization on sublattice B is still non-zero. Above T^* the system of equations (20) has no solution and one has to modify the spin-wave theory. The magnetization depends on the dimensionless temperature T/J and dimensionless parameters $s_1, s_2, J_1/J$ and J_2/J. For parameters $s_1 = 1.5, s_2 = 1, J_1/J = 0.94$ and $J_2/J = 0.01$ the functions $M^A(T/J)$ and $M^B(T/J)$ are depicted in figure 1. The upper (red) line is the sublattice A magnetization, while the bottom (blue) line is the sublattice B magnetization.

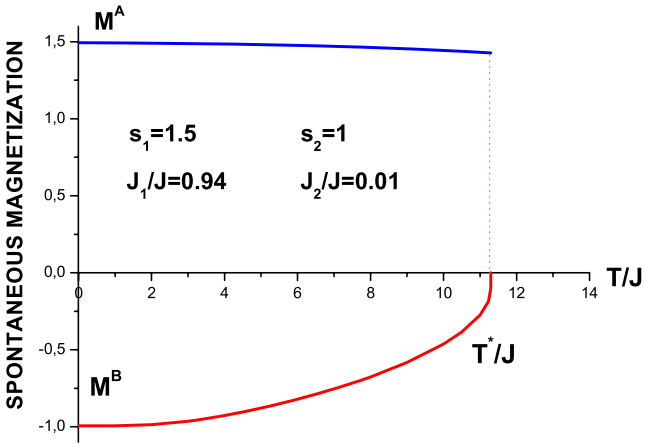

Figure 1. The spontaneous magnetization M^{A}—upper (red) line and M^{B}—bottom (blue) line as a function of T/J for parameters $s_1 = 1.5$, $s_2 = 1$, $J_1/J = 0.94$ and $J_2/J = 0.01$. T^* is the temperature at which sublattice B magnetization becomes equal to zero.

2.2. *Modified RSW theory*

Once suppressed, the sublattice B magnetization cannot be restored by increasing the temperature above T^*. To formulate this mathematically we modify the spin-wave theory using the idea of a description of the paramagnetic phase of 2D ferromagnets ($T > 0$) by means of modified spin-wave theory [10, 11] and its generalization [1]. We consider a two-sublattice system and, to enforce the magnetization on the two sublattices to be equal to zero in the paramagnetic phase, we introduce two parameters λ_{A} and λ_{B} [1]. The new Hamiltonian is obtained from the old one equation (1) by adding two new terms:

$$\hat{H} = H - \sum_{i\in \mathrm{A}} \lambda_1 S_{1i}^3 + \sum_{i\in \mathrm{B}} \lambda_2 S_{2i}^3. \tag{23}$$

In momentum space the new Hamiltonian adopts the form

$$\hat{H} = \sum_{k\in \mathrm{B_r}} [\hat{\varepsilon}_k^a a_k^+ a_k + \hat{\varepsilon}_k^b b_k^+ b_k - \gamma_k (b_k a_k + b_k^+ a_k^+)] \tag{24}$$

where the new dispersions are

$$\hat{\varepsilon}_k^a = \varepsilon_k^a + \lambda_1, \qquad \hat{\varepsilon}_k^b = \varepsilon_k^b + \lambda_2. \tag{25}$$

Utilizing the same transformation equations (13) with parameters

$$\hat{u}_k = \sqrt{\frac{1}{2}\left(\frac{\hat{\varepsilon}_k^a + \hat{\varepsilon}_k^b}{\sqrt{(\hat{\varepsilon}_k^a + \hat{\varepsilon}_k^b)^2 - 4\gamma_k^2}} + 1\right)}$$
$$\hat{v}_k = \mathrm{sgn}(\gamma_k) \sqrt{\frac{1}{2}\left(\frac{\hat{\varepsilon}_k^a + \hat{\varepsilon}_k^b}{\sqrt{(\hat{\varepsilon}_k^a + \hat{\varepsilon}_k^b)^2 - 4\gamma_k^2}} - 1\right)} \tag{26}$$

one obtains the Hamiltonian in diagonal form

$$\hat{H} = \sum_{k\in \mathrm{B_r}} (\hat{E}_k^\alpha \alpha_k^+ \alpha_k + \hat{E}_k^\beta \beta_k^+ \beta_k + \hat{E}_k^0), \tag{27}$$

where

$$\hat{E}_k^\alpha = \tfrac{1}{2}\left[\sqrt{(\hat{\varepsilon}_k^a + \hat{\varepsilon}_k^b)^2 - 4\gamma_k^2} - \hat{\varepsilon}_k^b + \hat{\varepsilon}_k^a\right]$$
$$\hat{E}_k^\beta = \tfrac{1}{2}\left[\sqrt{(\hat{\varepsilon}_k^a + \hat{\varepsilon}_k^b)^2 - 4\gamma_k^2} + \hat{\varepsilon}_k^b - \hat{\varepsilon}_k^a\right] \tag{28}$$
$$\hat{E}_k^0 = \tfrac{1}{2}\left[\sqrt{(\hat{\varepsilon}_k^a + \hat{\varepsilon}_k^b)^2 - 4\gamma_k^2} - \hat{\varepsilon}_k^b - \hat{\varepsilon}_k^a\right].$$

It is convenient to represent the parameters λ_1 and λ_2 in the form

$$\lambda_1 = 6Jus_2(\mu_1 - 1), \qquad \lambda_2 = 6Jus_1(\mu_2 - 1). \tag{29}$$

In terms of the new parameters μ_1 and μ_2 the dispersions $\hat{\varepsilon}_k^a$ and $\hat{\varepsilon}_k^b$ adopt the form

$$\hat{\varepsilon}_k^a = 4s_1 J_1 u_1 \varepsilon_k + 6s_2 Ju\mu_1$$
$$\hat{\varepsilon}_k^b = 4s_2 J_2 u_2 \varepsilon_k + 6s_1 Ju\mu_2. \tag{30}$$

They are positive ($\hat{\varepsilon}_k^a > 0$, $\hat{\varepsilon}_k^b > 0$) for all values of the wavevector k, if the parameters μ_1 and μ_2 are positive ($\mu_1 > 0, \mu_2 > 0$). The dispersion equations (28) are well defined if square roots in equations (28) are well defined. This is true if

$$\mu_1\mu_2 \geqslant 1. \tag{31}$$

The β_k excitation is gapped ($E_k^\beta > 0$) for all values of parameters μ_1 and μ_2 which satisfy equation (31). The α excitation is gapped if $\mu_1\mu_2 > 1$, but in the particular case

$$\mu_1\mu_2 = 1. \tag{32}$$

$\hat{E}_0^\alpha = 0$, and near the zero wavevector

$$\hat{E}_k^\alpha \approx \hat{\rho}k^2 \tag{33}$$

with the spin-stiffness constant

$$\hat{\rho} = \frac{8(s_2^2 J_2 u_2 \mu_1 + s_1^2 J_1 u_1 \mu_2) + 2s_1 s_2 Ju}{(s_1\mu_2 - s_2\mu_1)}. \tag{34}$$

In the particular case equation (32) the α_k boson is the long-range excitation (magnon) in the system.

We introduced the parameters λ_1 and λ_2 (μ_1, μ_2) to enforce the sublattice A and B spontaneous magnetizations to be equal to zero in the paramagnetic phase. We find out the parameters μ_1 and μ_2, as well as the Hartree–Fock parameters, as functions of temperature, solving the system of five equations, equations (20) and the equations $M^{\mathrm{A}} = M^{\mathrm{B}} = 0$, where the spontaneous magnetizations have the same representation as equations (22) but with coefficients $\hat{u}_k, \hat{v}_k$, and dispersions $\hat{E}_k^\alpha, \hat{E}_k^\beta$ in the expressions for the Bose functions. The numerical calculations show that for high enough temperature $\mu_1\mu_2 > 1$. When the temperature decreases the product $\mu_1\mu_2$ decreases, remaining larger than one. The temperature at which the product becomes equal to one ($\mu_1\mu_2 = 1$) is the Néel temperature. Below T_{N}, the spectrum contains long-range (magnon) excitations, thereupon $\mu_1\mu_2 = 1$. It is convenient to represent the parameters in the following way:

$$\mu_1 = \mu, \qquad \mu_2 = 1/\mu. \tag{35}$$

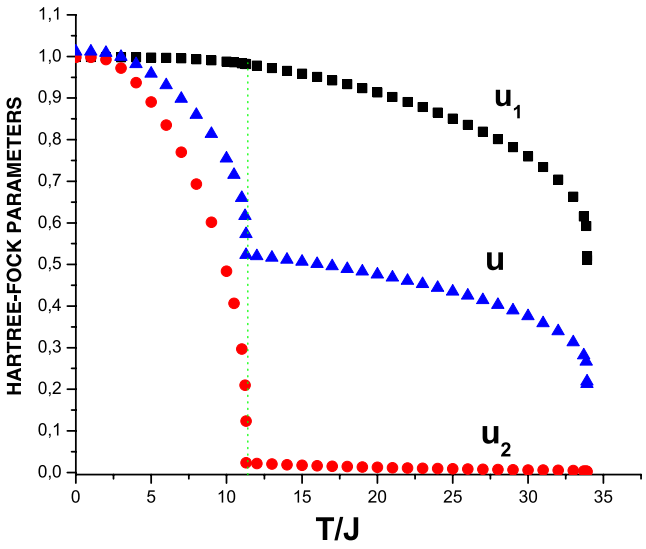

Figure 2. Hartree–Fock parameters u_1, u_2 and u as a function of T/J for $s_1 = 1.5$, $s_2 = 1$, $J_1/J = 0.94$ and $J_2/J = 0.01$. The vertical dotted (green) line corresponds to T^*/J.

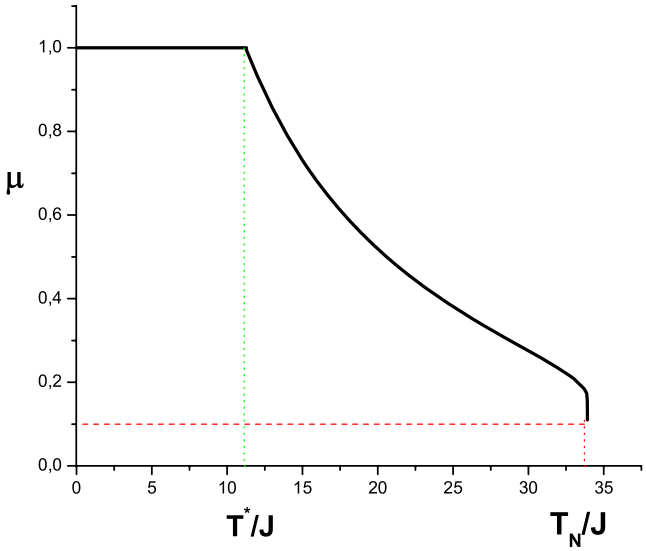

Figure 3. $\mu(T/J)$ for parameters $s_1 = 1.5$, $s_2 = 1$, $J_1/J = 0.94$ and $J_2/J = 0.01$. The vertical dotted (green) line corresponds to T^*/J, while (red) dashed lines to T_N/J and $\mu(T_N/J)$.

In the ordered phase magnon excitations are the origin of the suppression of the magnetization. Near zero temperature their contribution is small and at zero temperature sublattice A and B spontaneous magnetization reach their saturation. On increasing the temperature magnon fluctuations suppress the sublattice A magnetization and sublattice B magnetization in different ways. At T^* the sublattice B spontaneous magnetization becomes equal to zero. Increasing the temperature above T^*, the sublattice B magnetization should be zero. This is why we impose the condition $M^B(T) = 0$ if $T > T^*$. For temperatures above T^*, the parameter μ and the Hartree–Fock parameters are solutions of a system of four equations, equations (20) and the equation $M^B = 0$. The Hartree–Fock parameters, as a function of temperature

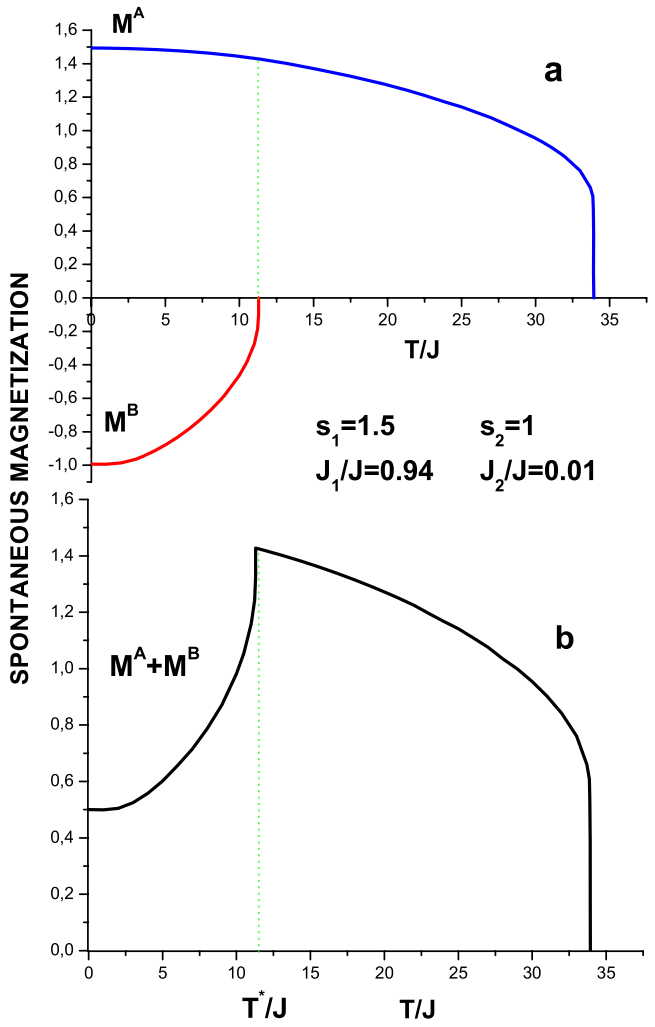

Figure 4. (a) The sublattice A spontaneous magnetization M^A—upper (blue) line and sublattice B spontaneous magnetization M^B—bottom (red) line as a function of T/J for parameters $s_1 = 1.5$, $s_2 = 1$, $J_1/J = 0.94$ and $J_2/J = 0.01$. (b) The total spontaneous magnetization $M^A + M^B$. T^*/J—vertical dotted (green) line.

T/J, are depicted in figure 2 for parameters $s_1 = 1.5$, $s_2 = 1$, $J_1/J = 0.94$ and $J_2/J = 0.01$. The vertical dotted (green) line corresponds to T^*/J.

The function $\mu(T/J)$ is depicted in figure 3 for the same parameters.

We utilize the obtained function $\mu(T)$, $u_1(T)$, $u_2(T)$, $u(T)$ to calculate the spontaneous magnetization as a function of the temperature. Above T^*, the magnetization of the system is equal to the sublattice A magnetization. For the same parameters as above the functions $M^A(T/J)$ and $M^B(T/J)$ are depicted in figure 4(a). The upper (blue) line is the sublattice A magnetization, while the bottom (red) line is the sublattice B magnetization. The total magnetization $M = M^A + M^B$ is depicted in figure 4(b).

3. T_N and T^* dependence on model's parameters

The existence of two ferromagnetic phases $(0, T^*)$ and (T^*, T_N) is a generic feature of two-spin systems. The

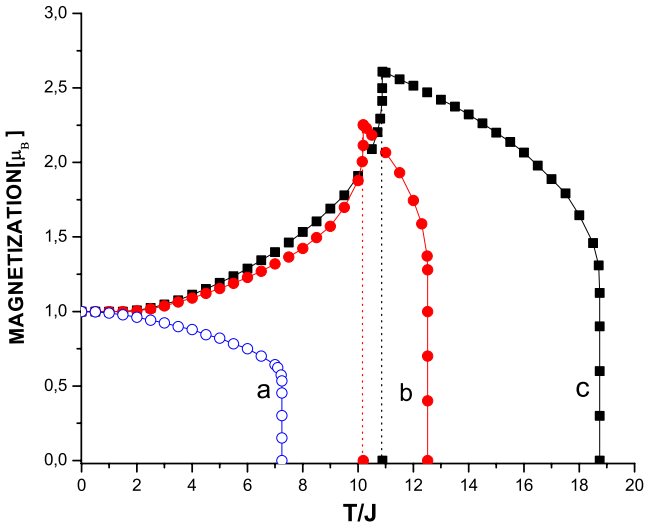

Figure 5. The magnetization $2M^{\mathrm{A}} + 2M^{\mathrm{B}}$ as a function of T/J for $s_1 = 1.5$ and $s_2 = 1$. Curve a: $J_1/J = 0.05$, $J_2/J = 0.0005$, curve b: $J_1/J = 0.3$, $J_2/J = 0.003$, curve c: $J_1/J = 0.5$, $J_2/J = 0.005$.

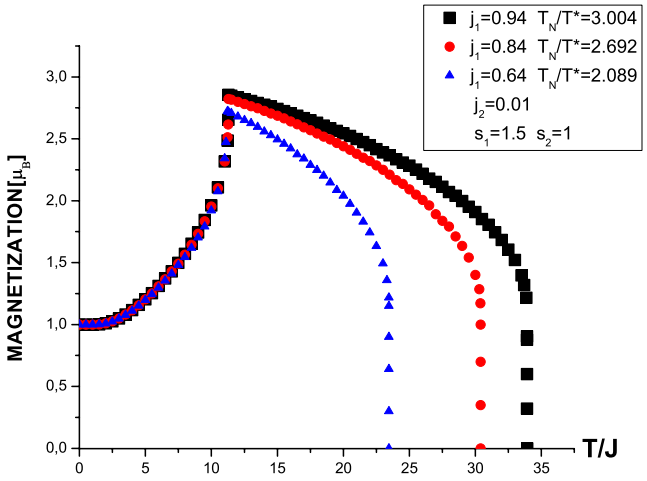

Figure 6. The magnetization $2M^{\mathrm{A}} + 2M^{\mathrm{B}}$ as a function of T/J for $s_1 = 1.5$, $s_2 = 1$, $j_2 = J_2/J = 0.01$ and three values of the parameter $j_1 = J_1/J$; $j_1 = 0.94$ (black) squares, $j_1 = 0.84$ (red) circles and $j_1 = 0.64$ (blue) triangles.

characteristic temperatures T_{N} and T^* strongly depend on the parameters of the model. Intuitively, it is clear that, if the inter-exchange is much stronger than intra-exchange, the ferromagnetic order sets in simultaneously on both sublattices. This is not true, if inter-exchange is not so strong. To demonstrate this I study a system with sublattice A spin $s_1 = 1.5$ and sublattice B spin $s_2 = 1$. For the parameters $J_1/J = 0.5$ and $J_2/J = 0.005$ the magnetization–temperature curve is depicted in figure 5 curve 'c'. The ratio of the characteristic temperatures equals $T_{\mathrm{N}}/T^* = 1.722$. Increasing the inter-exchange coupling, $J_1/J = 0.3$, $J_2/J = 0.003$ (curve 'b'), the ratio decreases, $T_{\mathrm{N}}/T^* = 1.229$, and above some critical value of the inter-exchange constant $J_1/J = 0.05$, $J_2/J = 0.0005$ Néel's temperature becomes equal to T^*. There is only one ferromagnetic phase and magnetization–temperature curve 'a' is a typical Curie–Weiss curve. Despite this the system does not describe a ferromagnet, because the spin-wave excitations are superpositions of the sublattice A and B spin excitations.

Next, I consider a system with sublattice A spin $s_1 = 1.5$ and sublattice B spin $s_2 = 1$. The ratio of sublattice B exchange constant J_2 and inter-exchange constant J is fixed $j_2 = J_2/J = 0.01$, while the ratio $j_1 = J_1/J$ varies. When the sublattice A exchange constant J_1 increases $j_1 = J_1/J = 0.64, 0.84$ and 0.94, the magnetization–temperature curve at temperatures below T^* does not change. There is no visible difference between T^* temperatures for the three values of the parameter J_1/J. The difference appears when the temperature is above T^*. Increasing the sublattice A exchange constant increases the Néel temperature. The three curves are depicted in figure 6.

Finally, I consider three systems with equal exchange constants $J_1/J = 0.4$, $J_2/J = 0.004$ and sublattice A spin $s_1 = 4$, but with three different sublattice B spins (figure 7). The calculations show that decreasing the sublattice B spin decreases the T^* temperature, increases the maximum of magnetization at T^* and zero temperature magnetization.

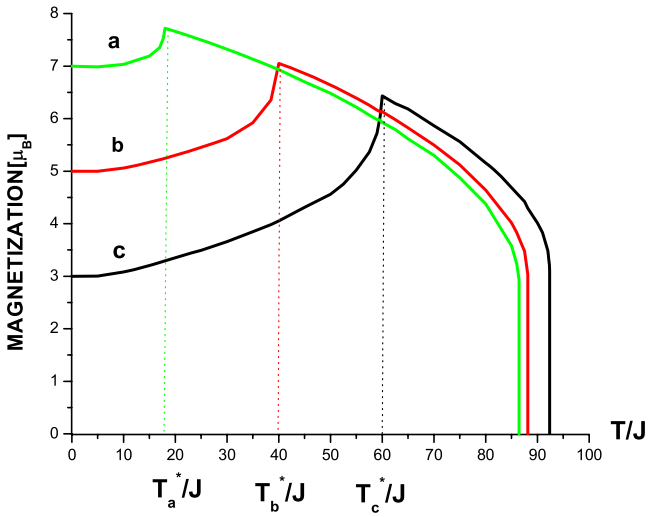

Figure 7. The magnetization $2M^{\mathrm{A}} + 2M^{\mathrm{B}}$ as a function of T/J for $J_1/J = 0.4$, $J_2/J = 0.004$, $s_1 = 4$ and $s_2 = 0.5$—curve a (green), $s_2 = 1.5$—curve b (red), $s_2 = 2.5$—curve c (black).

4. Theory and experiment

4.1. Sulfo-spinel $MnCr_2S_{4-x}Se_x$

The sulfo-spinel $MnCr_2S_{4-x}Se_x$ has been investigated by measurements of the magnetization at 15.3 kOe as a function of temperature (figure 94 in [4]). The maximum in the magnetization versus temperature curve, which is typical of $MnCr_2S_4$ ($x = 0$), increases when x increases and disappears at $x = 0.5$. The Néel temperature decreases from 74 K at $x = 0$ to 56 K at $x = 2$. The authors' conclusion is that the observed change of the magnetic properties is attributed to a decrease of the strength of the negative Mn^{2+}–Cr^{3+} superexchange interaction with increasing Se concentration.

We obtained, see figure 5, that the maximum of the magnetization is at T^*. Above T^* the magnetization of the

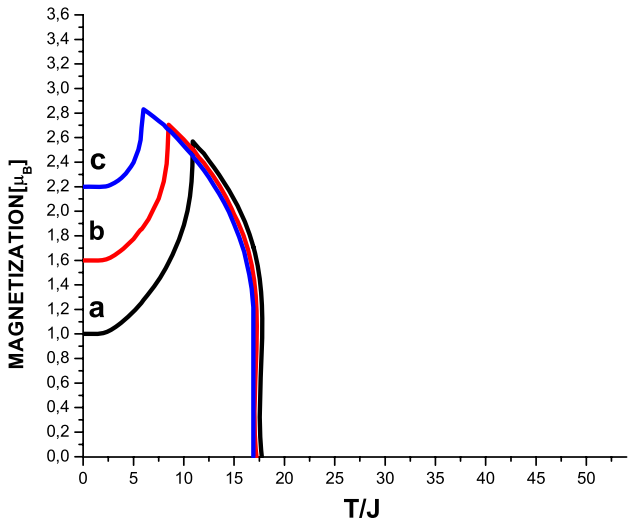

Figure 8. The magnetization $2M^{\mathrm{A}} + 2M^{\mathrm{B}}$ as a function of T/J for $J_1/J = 0.47$, $J_2/J = 0.001$, $s_1 = 1.5$ and $s_2 = 1$—curve a (black), $s_2 = 0.7$—curve b (red), $s_2 = 0.4$—curve c (blue).

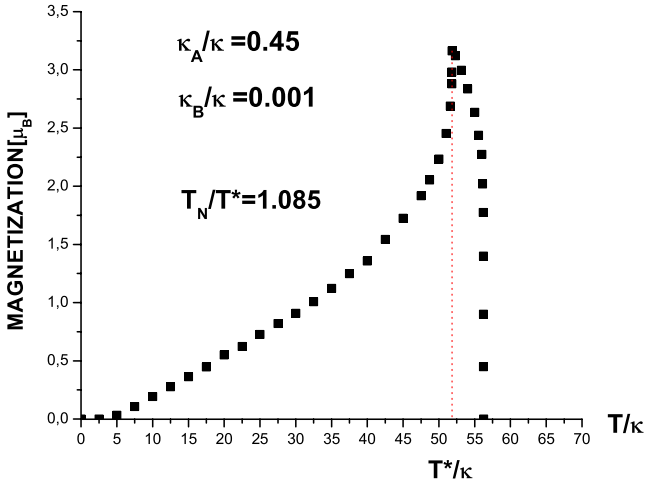

Figure 9. The magnetization $g_{\mathrm{A}}M^{\mathrm{A}} + g_{\mathrm{B}}M^{\mathrm{B}}$ as a function of T/κ for parameters $\kappa_{\mathrm{A}}/\kappa = 0.45$ and $\kappa_{\mathrm{B}}/\kappa = 0.001$.

system is equal to the magnetization of sublattice A spins. If we extrapolate this curve below T^* down to zero temperature we will obtain a value close to $2s_1\mu_{\mathrm{B}}$, where s_1 is the spin of the sublattice A spin operators. The experimental figures [4] show that extrapolations give one and the same result for all values of x. One can accept the fact that the Se concentration does not influence the value of the sublattice A spin and $s_1 = 1.5$.

Below T^* the magnetization is a sum of sublattice A and B magnetization. Hence, the magnetization at zero temperature is equal to $2(s_1 - s_2)\mu_{\mathrm{B}}$. Therefore, one can determine the sublattice B spin s_2. The results of the theoretical calculations of magnetization, in Bohr magnetons, are depicted in figure 8 for parameters $s_1 = 1.5$, $J_1/J = 0.47$, $J_2/J = 0.001$ and $s_2 = 1$—curve a (black); $s_2 = 0.7$—curve b (red) and $s_2 = 0.4$—curve c (blue). The temperature and magnetization axes are chosen in accordance with the experimental figure. Comparing figure 94 in [4] and figure 6 in the present paper, one concludes that the effective sublattice B spin s_2 decreases with increasing Se concentration, and this is the origin of the anomalous temperature variation of magnetization. Figure 8 shows that the present calculations capture the essential features of the system; increasing the Se concentration (decreasing s_2) leads to a decrease of Néel temperature, the T^* temperature decreases too, and the maximum of the magnetization increases. Comparing figure 8 in the present paper and figure 5 in [1] one realizes the importance of the present method of calculation for adequately reproducing the characteristic temperatures T_{N}, T^* and the shape of the magnetization–temperature curves.

4.2. *Vanadium spinel MnV_2O_4*

The spinel MnV_2O_4 is a two-sublattice ferrimagnet, with site A occupied by the Mn^{2+} ion, which is in the $3d^5$ high-spin configuration with quenched orbital angular momentum, which can be regarded as a simple $s = 5/2$ spin. The B site is occupied by the V^{3+} ion, which takes the $3d^2$ high-spin configuration in the triply degenerate t_{2g} orbital and has orbital degrees of freedom. The measurements show that the setting in of the magnetic order is at the Néel temperature $T_{\mathrm{N}} = 56.5$ K [5] and that the magnetization has a maximum near $T^* = 53.5$ K. Below this temperature the magnetization sharply decreases and goes to zero when the temperature approaches zero.

We consider a system which obtains its magnetic properties from Mn and V magnetic moments. Because of the strong spin–orbital interaction it is convenient to consider jj coupling with $\mathbf{J}^{\mathrm{A}} = \mathbf{S}^{\mathrm{A}}$ and $\mathbf{J}^{\mathrm{B}} = \mathbf{L}^{\mathrm{B}} + \mathbf{S}^{\mathrm{B}}$. The sublattice A total angular momentum is $j_{\mathrm{A}} = s_{\mathrm{A}} = 5/2$, while the sublattice B total angular momentum is $j_{\mathrm{B}} = l_{\mathrm{B}} + s_{\mathrm{B}}$, with $l_{\mathrm{B}} = 3$ and $s_{\mathrm{B}} = 1$ [5]. Then the g factor for sublattice A is $g_{\mathrm{A}} = 2$ and the atomic value of g_{B} is $g_{\mathrm{B}} = \frac{5}{4}$. The sublattice A magnetic order is antiparallel to the sublattice B one and the saturated magnetization is $\sigma = 2\frac{5}{2} - \frac{5}{4}4 = 0$, in agreement with the experimental finding that the magnetization goes to zero when the temperature approaches zero. The Hamiltonian of the system is

$$H = -\kappa_{\mathrm{A}} \sum_{\langle\langle ij\rangle\rangle_{\mathrm{A}}} \mathbf{J}_i^{\mathrm{A}} \cdot \mathbf{J}_j^{\mathrm{A}} - \kappa_{\mathrm{B}} \sum_{\langle\langle ij\rangle\rangle_{\mathrm{B}}} \mathbf{J}_i^{\mathrm{B}} \cdot \mathbf{J}_j^{\mathrm{B}} + \kappa \sum_{\langle ij\rangle} \mathbf{J}_i^{\mathrm{A}} \cdot \mathbf{J}_j^{\mathrm{B}}. \quad (36)$$

The first two terms describe the ferromagnetic Heisenberg intra-sublattice exchange $\kappa_{\mathrm{A}} > 0, \kappa_{\mathrm{B}} > 0$, while the third term describes the inter-sublattice exchange which is antiferromagnetic $\kappa > 0$. To proceed we use the Holstein–Primakoff representation of the total angular momentum vectors $\mathbf{J}_j^{\mathrm{A}}(a_j^+, a_j)$ and $\mathbf{J}_j^{\mathrm{B}}(b_j^+, b_j)$, where a_j^+, a_j and b_j^+, b_j are Bose fields, and repeat the calculations from sections 2 and 3. The magnetization of the system $g_{\mathrm{A}}M^{\mathrm{A}} + g_{\mathrm{B}}M^{\mathrm{B}}$ as a function of temperature is depicted in figure 9 for parameters $\kappa_{\mathrm{A}}/\kappa = 0.45$ and $\kappa_{\mathrm{B}}/\kappa = 0.001$. The parameters are chosen so that the calculations reproduce the experimental value of the ratio T_{N}/T^*.

The profile of the magnetization–temperature curve is in very good agreement with the experimental zero-field-cooling (ZFC) magnetization curves [6, 7]. The anomalous

temperature dependence of the magnetization is reproduced, but there is an important difference between the interpretation of the experimental results in [5–9] and the present theoretical results. In the experimental papers T_N is the temperature at which both the Mn and V magnetization become equal to zero. The present theory predicts two phases: at low temperatures $(0, T^*)$ sublattice Mn magnetization and sublattice V magnetization contribute to the magnetization of the system, while at high temperatures (T^*, T_N) only Mn ions have non-zero spontaneous magnetization. The vanadium sublattice magnetization set in at T^*, and evidence for this is the abrupt decrease of magnetization below T^*, which also indicates that the magnetic order of vanadium electrons is antiparallel to the order of Mn electrons.

For samples cooled in a field (FC magnetization) the field leads to the formation of a single domain and, in addition, increases the chaotic order of the spontaneous magnetization of the vanadium sublattice, which is antiparallel to it. As a result the average value of the vanadium magnetic order decreases and does not compensate the *Mn* magnetic order. The magnetization curves depend on the applied field, and do not go to zero. For a larger field the (FC) curve increases when temperature decreases below the Néel temperature. It has a maximum at the same temperature $T^* < T_N$ as the ZFC magnetization and a minimum at $T_1^* < T^*$. Below T_1^* the magnetization increases monotonically when the temperature approaches zero.

The experiments with samples cooled in a field (FC magnetization) provide a new opportunity to clarify the magnetism of the manganese vanadium oxide spinel. The applied field is antiparallel to the vanadium magnetic moment and strongly affect it. On the other hand, the experiments show that there is no difference between ZFC and FC magnetization curves when the temperature runs over the interval (T^*, T_N) [6, 7]. They begin to diverge when the temperature is below T^*. This is in accordance with the theoretical prediction that the vanadium magnetic moment does not contribute to magnetization when $T > T^*$ and T^* is the temperature at which the vanadium ions start to contribute the magnetization of the system. Because of the strong field, the two vanadium bands are split and the magnetic moment of one of the t_{2g} electrons is reoriented to be parallel with the field and magnetic order of the Mn electrons. The description of this case is more complicated and requires three magnetic orders to be involved. When $T^* < T < T_N$ only Mn ions have non-zero spontaneous magnetization. At T^* vanadium magnetic order antiparallel to the magnetic order of Mn sets in and partially compensates it. Below T_1^* the reoriented electron gives a contribution, which explains the increasing magnetization of the system when the temperature approaches zero. A series of experiments with different applied fields could be decisive for the confirmation or rejection of the T^* transition. Increasing the applied field one expects an increase of T_1^* and when the field is strong enough, so that all vanadium electrons are reoriented, an anomalous increasing of magnetization below T^* would be obtained as within the ferromagnetic phase of UGe_2 [12].

5. Summary

In summary, I have worked out a renormalized spin-wave theory and its extension to describe the two phases $(0, T^*)$ and (T^*, T_N) of a two-sublattice ferrimagnet. Comparing figure 4 in the present paper and figure 4 in [1], and figure 8 in the present paper and figure 5 in [1], one becomes aware of the relevance of the present calculations for the accurate reproduction of the basic features of the system near the characteristic temperatures T_N and T^*.

The present theory of ferrimagnetism permits us to consider more complicated systems such as the $CeCrSb_3$ compound [13] or the spinel Fe_3O_4 which are two-sublattice ferrimagnets but with three spins.

Acknowledgment

This work was partly supported by a Grant-in-Aid DO02-264/18.12.08 from NSF-Bulgaria.

Appendix

To make more transparent the derivation of the equations for the Hartree–Fock parameters (equations (20)) I consider the first term (the sublattice A term) in the Hamiltonian of the magnon–magnon interaction equation (6). To write this term in the Hartree–Fock approximation one represents the product of two Bose operators in the form

$$a_i^+ a_j = a_i^+ a_j - \langle a_i^+ a_j\rangle + \langle a_i^+ a_j\rangle \tag{A.1}$$

and neglects all terms $(a_i^+ a_j - \langle a_i^+ a_j\rangle)^2$ in the four-magnon interaction Hamiltonian. The result is

$$\begin{aligned}
&\tfrac{1}{2}a_i^+ a_j a_i^+ a_i \approx -\langle a_i^+ a_j\rangle\langle a_i^+ a_i\rangle + \langle a_i^+ a_j\rangle a_i^+ a_i + a_i^+ a_j\langle a_i^+ a_i\rangle\\
&\tfrac{1}{2}a_j^+ a_i a_j^+ a_j \approx -\langle a_j^+ a_i\rangle\langle a_j^+ a_j\rangle + \langle a_j^+ a_i\rangle a_j^+ a_j + a_j^+ a_i\langle a_j^+ a_j\rangle\\
&\tfrac{1}{2}a_j^+ a_j a_i^+ a_j \approx -\langle a_j^+ a_j\rangle\langle a_i^+ a_j\rangle + \langle a_j^+ a_j\rangle a_i^+ a_j\\
&\qquad + a_j^+ a_j\langle a_r^+ a_j\rangle\\
&a_i^+ a_i a_j^+ a_j \approx -\langle a_i^+ a_i\rangle\langle a_j^+ a_j\rangle + \langle a_i^+ a_i\rangle a_j^+ a_j + a_i^+ a_i\langle a_j^+ a_j\rangle\\
&\qquad - \langle a_i^+ a_j\rangle\langle a_j^+ a_i\rangle + \langle a_i^+ a_j\rangle a_j^+ a_i + a_j^+ a_i\langle a_i^+ a_j\rangle.
\end{aligned} \tag{A.2}$$

The Hartree–Fock approximation of the sublattice A part of the Hamiltonian of the magnon–magnon interaction is

$$\begin{aligned}
&\tfrac{1}{4}J_1\sum_{\langle\langle ij\rangle\rangle_A}[a_i^+ a_j^+(a_i - a_j)^2 + (a_i^+ - a_j^+)^2 a_i a_j]\\
&\quad\approx 12NJ_1 s_1^2(u_1 - 1)^2 + J_1 s_1(u_1 - 1)\\
&\quad\times\sum_{\langle\langle ij\rangle\rangle_A}(a_i^+ a_i + a_j^+ a_j - a_j^+ a_i - a_i^+ a_j)
\end{aligned} \tag{A.3}$$

where the Hartree–Fock parameter u_1 is defined by the equation

$$u_1 = 1 - \frac{1}{6s_1}\frac{1}{N}\sum_{k\in B_r} e_k\langle a_k^+ a_k\rangle. \tag{A.4}$$

Combining the sublattice A part of the Hamiltonian equation (5) (the first term) and equation (A.3) one obtains the

Hartree–Fock approximation for the sublattice A part of the Hamiltonian:

$$H^{\mathrm{A}} \approx 12NJ_1 s_1^2(u_1-1)^2 + J_1 s_1 u_1 \times \sum_{\langle\langle ij\rangle\rangle_{\mathrm{A}}} (a_i^+ a_i + a_j^+ a_j - a_j^+ a_i - a_i^+ a_j). \quad (A.5)$$

In the same way one obtains the Hartree–Fock approximation of the sublattice B and inter-sublattices parts of the Hamiltonian. The result is the H_{HF} Hamiltonian equations (7)–(9).

To calculate the thermal average $\langle a_k^+ a_k\rangle$, in equation (A.4), one utilizes the Hamiltonian H_{HF}. Therefore, the matrix element depends on the Hartree–Fock parameters, and equation (A.4) is one of the self-consistent equations for these parameters.

The matrix element can be represented in terms of $\alpha_k(\alpha_k^+)$ and $\beta_k(\beta_k^+)$ equations (13):

$$\langle a_k^+ a_k\rangle = u_k^2 n_k^\alpha + v_k^2 n_k^\beta + v_k^2 \quad (A.6)$$

where $n_k = \langle\alpha_k^+\alpha_k\rangle$, $\langle\beta_k^+\beta_k\rangle$ are the Bose functions of α and β excitations. Substituting the thermal average in equation (A.4) with equation (A.6), one obtains that equation (A.4) is exactly the first equation of the system equations (20) which in turn is obtained from the first of the equations (19).

References

[1] Karchev N 2008 *J. Phys.: Condens. Matter* **20** 325219
[2] Mermin N D and Wagner H 1966 *Phys. Rev. Lett.* **17** 1133
[3] Néel L 1948 *Ann. Phys., Paris* **3** 137
[4] Van Stapele P P 1982 *Handbook of Magnetic Materials* vol 3, ed E P Wohlfarth (Amsterdam: North-Holland) p 603
[5] Adachi K, Suzuki T, Kato K, Osaka K, Takata M and Katsufuji T 2005 *Phys. Rev. Lett.* **95** 197202
[6] Garlea V O, Jin R, Mandrus D, Roessli B, Huang Q, Miller M, Schultz A J and Nagler S E 2008 *Phys. Rev. Lett.* **100** 066404
[7] Baek S-H, Choi K-Y, Reyes A P, Kuhns P L, Curro N J, Ramanchandran V, Dalal N S, Zhou H D and Wiebe C R 2008 *J. Phys.: Condens. Matter* **20** 135218
[8] Zhou H D, Lu J and Wiebe C R 2007 *Phys. Rev.* B **76** 174403
[9] Hardy V, Bréard Y and Martin C 2008 *Phys. Rev.* B **78** 024406
[10] Takahashi M 1986 *Prog. Theor. Phys. Suppl.* **87** 233
[11] Takahashi M 1987 *Phys. Rev. Lett.* **58** 168
[12] Pfleiderer C and Huxley A D 2002 *Phys. Rev. Lett.* **89** 147005
[13] Jackson D D, McCall S K, Karki A B and Young D P 2007 *Phys. Rev.* B **76** 064408